



## Structure-based engineering of benzalacetone synthase

Yoshihiko Shimokawa, Hiroyuki Morita, Ikuro Abe\*

Graduate School of Pharmaceutical Sciences, The University of Tokyo, 7-3-1 Hongo, Bunkyo-ku, Tokyo 113-0033, Japan

### ARTICLE INFO

#### Article history:

Received 17 June 2010

Revised 4 July 2010

Accepted 7 July 2010

Available online 11 July 2010

#### Keywords:

Polyketide synthase

Benzalacetone synthase

Enzyme

Site-directed mutagenesis

Enzyme engineering

### ABSTRACT

Benzalacetone synthase (BAS) and chalcone synthase (CHS) are plant-specific type III polyketide synthases (PKSs), sharing 70% amino acid sequence identity and highly homologous overall protein structures. BAS catalyzes the decarboxylative coupling of 4-coumaroyl-CoA with malonyl-CoA to produce the diketide benzalacetone, whereas CHS produces the tetraketide chalcone by iterative condensations with three molecules of malonyl-CoA, and folding the resulting intermediate into a new aromatic ring system. Recent crystallographic analyses of *Rheum palmatum* BAS revealed that the characteristic substitution of Thr132 (numbering of *Medicago sativa* CHS2), a conserved CHS residue lining the active-site cavity, with Leu causes steric contraction of the BAS active-site to produce the diketide, instead of the tetraketide. To test this hypothesis, we constructed a set of *R. palmatum* BAS site-directed mutants (L132G, L132A, L132S, L132C, L132T, L132F, L132Y, L132W and L132P), and investigated the mechanistic consequences of the point mutations. As a result, the single amino acid substitution L132T restored the chalcone-forming activity in BAS, whereas the Ala, Ser, and Cys substitutions expanded the product chain length to produce 4-coumaroyltriacetic acid lactone (CTAL) after three condensations with malonyl-CoA, but without the formation of the aromatic ring system. Homology modeling suggested that this is probably caused by the restoration of the 'coumaroyl binding pocket' in the active-site cavity. These findings provide further insights into the structural details of the catalytic mechanism of the type III PKS enzymes.

© 2010 Elsevier Ltd. All rights reserved.

Benzalacetone synthase (BAS), a member of the plant-specific chalcone synthase (CHS) superfamily of type III polyketide synthases (PKSs),<sup>1–3</sup> produces the diketide benzalacetone by the condensation of 4-coumaroyl-CoA with one molecule of malonyl-CoA (Figs. 1 and 2).<sup>4–7</sup> BAS generates the C<sub>6</sub>–C<sub>4</sub> scaffold of the biologically active phenylbutanoids, including raspberry ketone in raspberry fruit and the anti-inflammatory glucoside lindleyin in rhubarb.<sup>4</sup> In contrast, CHS, which shares ca. 70% amino acid sequence identity with BAS, catalyzes iterative condensations of 4-coumaroyl-CoA with three molecules of malonyl-CoA, and folds the resulting tetraketide intermediate into a new aromatic ring system to produce naringenin chalcone (Figs. 1 and 2).<sup>1–3</sup> Recent crystallographic and site-directed mutagenesis studies have begun to reveal that the functional diversity of the CHS-superfamily type III PKSs principally arises from simple steric modulations of the active-site architecture.<sup>8–18</sup>

We previously reported the cloning and characterization of BAS from rhubarb (*Rheum palmatum*),<sup>4–6</sup> and solved the X-ray crystal structures of both the wild-type and chalcone-producing I214L/L215F mutant (numbering of *Medicago sativa* CHS2).<sup>7</sup> The crystal

structures at 1.8 Å resolution revealed that BAS utilizes an alternative, novel active-site pocket to bind the aromatic moiety of the coumarate, instead of CHS's 'coumaroyl binding pocket', which is lost in the active-site of the wild-type BAS and restored in the chalcone-producing double mutant (Fig. 3a and c).<sup>7</sup> In addition to the residues Ile214/Leu215, which are located at the junction between the active-site cavity and the CoA binding tunnel, the crystal structures suggested that the active-site residue Leu132, corresponding to Thr132 in CHS, at the entrance of the 'coumaroyl binding pocket', also plays an important role in the benzalacetone-forming activity. To test this hypothesis, and to clarify the structure–function relationships of the type III PKS enzymes, we constructed a set of site-directed mutants of *R. palmatum* BAS (L132G, L132A, L132S, L132C, L132T, L132F, L132Y, L132W and L132P), and investigated the mechanistic consequences of the point mutations.

The point mutants were expressed in *Escherichia coli* as GST-tagged fusion proteins, at levels comparable to that of the wild-type enzyme.<sup>19</sup> The recombinant enzymes were then purified to homogeneity by Glutathione Sepharose 4B affinity column, and the GST-tags were removed by digestion with PreScission Protease.<sup>20</sup> All of the mutants maintained the benzalacetone-forming activities at pH 8.0, whereas at pH 6.5, the point mutants afforded the triketide pyrone bisnoryangonin (BNY), after two condensations with malonyl-CoA, as in the case of the wild-type enzyme (Fig. 4).<sup>21,22</sup> It should be noted that, as previously reported, *R. palmatum* BAS shows pH dependency of the enzyme activity; the

Abbreviations: BAS, benzalacetone synthase; CHS, chalcone synthase; PKS, polyketide synthase; STS, stilbene synthase; BNY, bisnoryangonin; CTAL, 4-coumaroyltriacetic acid lactone.

\* Corresponding author. Tel.: +81 3 5841 4740; fax: +81 3 5841 4744.

E-mail address: [abe@mof.f.u-tokyo.ac.jp](mailto:abe@mof.f.u-tokyo.ac.jp) (I. Abe).

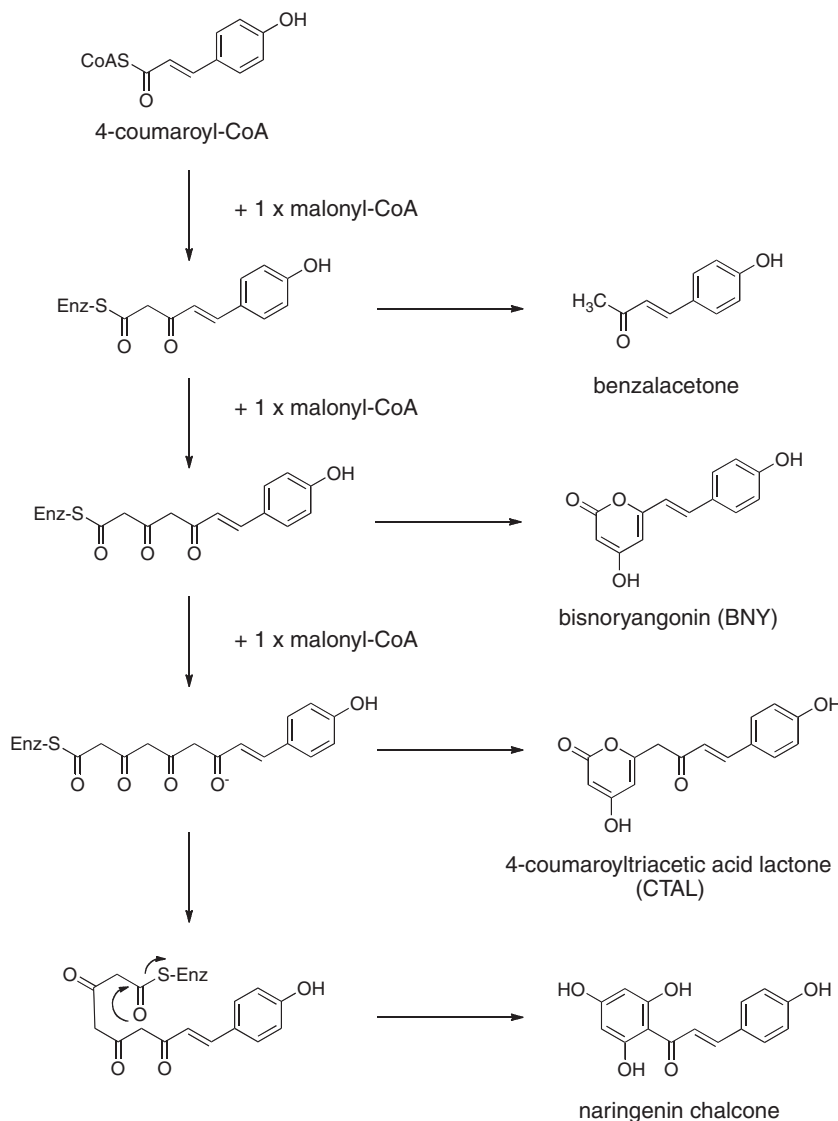


**Figure 1.** Proposed mechanism for the formation of benzalacetone, bisnoryangonin (BNY), 4-coumaroyltriacetic acid lactone (CTAL), naringenin chalcone and resveratrol from 4-coumaroyl-CoA and malonyl-CoA.

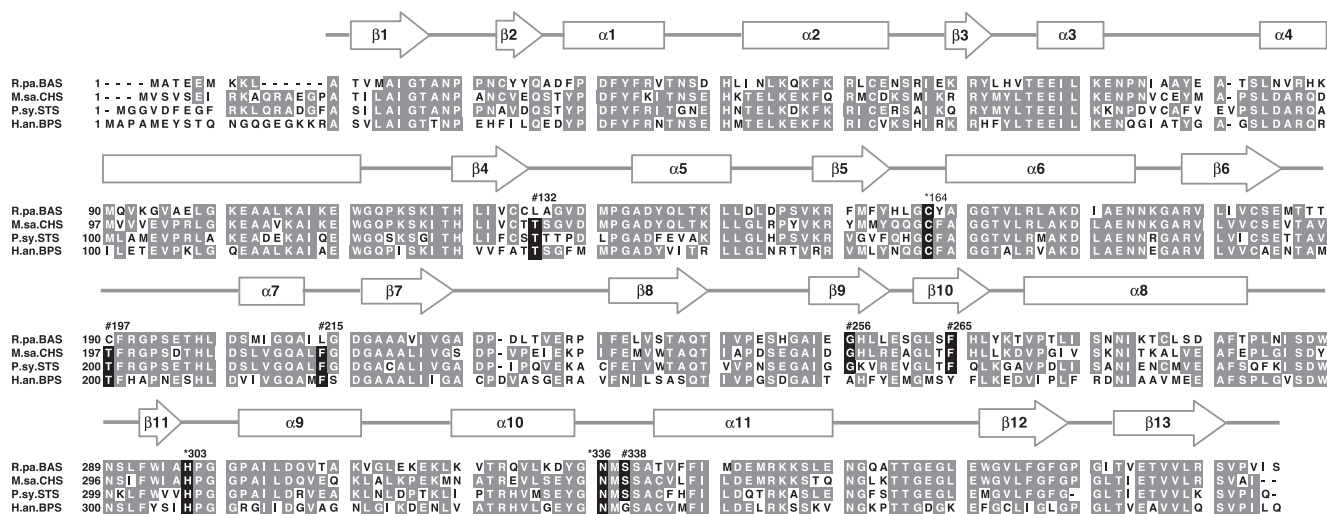


**Figure 2.** Comparison of the primary sequences of BAS and other type III PKSs. The secondary structures,  $\alpha$ -helices (rectangles),  $\beta$ -strands (arrows), and loops (bold lines), of BAS are also displayed. The catalytic triad Cys-His-Asn, and the residues considered to be crucial for the functional diversity of the type III PKSs are marked with \* and #, respectively. Abbreviations (GenBank accession numbers): R.pa.BAS, *Rheum palmatum* BAS (AAK82824); M.sa.CHS, *M. sativa* CHS (P30074); P.sy. STS, *Pinus sylvestris* STS (AAB24341); H.an. BPS, *Hypericum androsaemum* BPS (AAL79808).

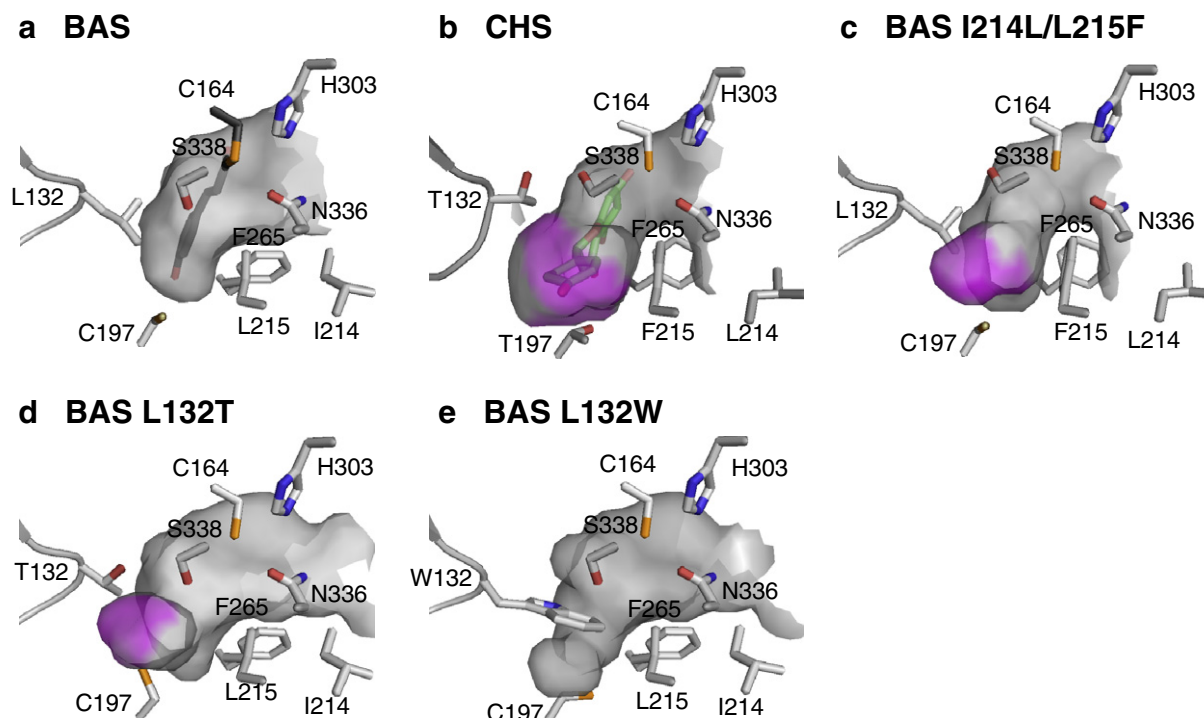


**Figure 3.** Comparison of the active-site architecture of (a) wild-type BAS, (b) *M. sativa* CHS, (c) the BAS I214L/L215F mutant, (d) the BAS L132T mutant, and (e) the BAS L132W mutant. The active-sites are represented by surface models. The coumarate that covalently binds to the active-site Cys in BAS and the naringenin molecules are shown as black and green stick models, respectively. The bottoms of the 'coumaroyl binding pocket' are highlighted in purple.

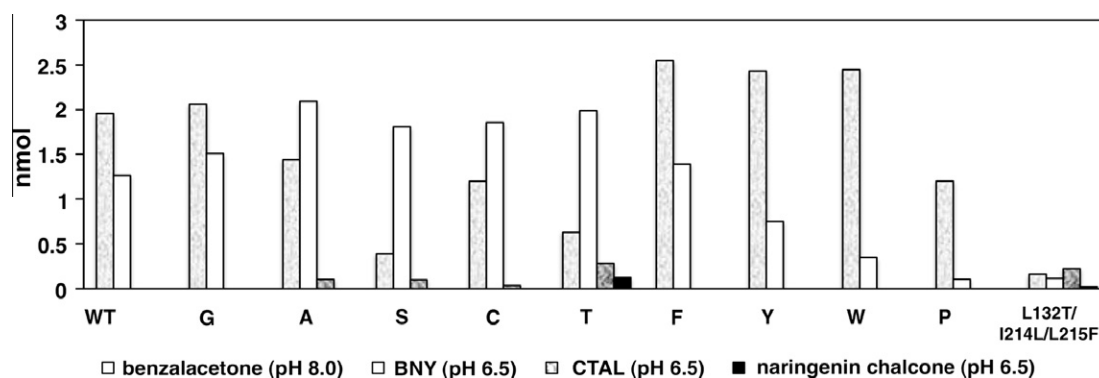


**Figure 4.** Production of benzalacetone (at pH 8.0), BNY (at pH 6.5), CTAL (at pH 6.5) and naringenin chalcone (at pH 6.5) by wild-type BAS and its mutants.

benzalacetone-forming activity is maximum within the pH 8.0–8.5 range, whereas under acidic conditions, BNY formation is dominant, and it is obtained almost as a single product at pH 6.5.<sup>5</sup> Remarkably, only the L132T mutant, in which Leu132 was substituted with Thr, as in the case of CHS, restored the chalcone-forming activity, to produce naringenin chalcone after three condensations with malonyl-CoA and the formation of the aromatic ring system. The L132T mutant also produced the tetraketide pyrone 4-coumaroyltriacetic acid lactone (CTAL) after three condensations with malonyl-CoA, along with BNY and benzalacetone (Fig. 4). The yields of benzalacetone, BNY, CTAL, and naringenin chalcone were 2.3%, 7.4%, 1.0%, and 0.5%, respectively. On the other hand, except for the L132G mutant, large-to-small substitutions with Ala, Ser, and Cys expanded the product chain length to yield CTAL after three condensations with malonyl-CoA, but without the formation of the aromatic ring system (Fig. 4). It was thus confirmed that the residue 132, located at the entrance of the 'coumaroyl binding pocket', indeed plays a critical role in the diketide formation reaction, along with the previously

reported active-site residues Leu215 and Ser338.<sup>5,6</sup> This is the first demonstration that a single amino acid replacement restored the chalcone-forming activity in *R. palmatum* BAS.

A steady-state kinetics analysis revealed that the BAS L132T mutant showed a  $K_M = 4.1 \mu\text{M}$  and a  $k_{\text{cat}} = 1.60 \times 10^{-3} \text{ min}^{-1}$  for 4-coumaroyl-CoA, with respect to the chalcone-forming activity, with a pH optimum of 6.5.<sup>23</sup> On the other hand, the previously reported chalcone-forming BAS I214L/L215F double mutant exhibited a  $K_M = 33.5 \mu\text{M}$  and a  $k_{\text{cat}} = 1.69 \times 10^{-1} \text{ min}^{-1}$  for 4-coumaroyl-CoA, representing a 13-fold increase in the  $k_{\text{cat}}/K_M$  value,<sup>5</sup> whereas the BAS wild-type enzyme showed a  $K_M = 10.0 \mu\text{M}$  and a  $k_{\text{cat}} = 1.79 \text{ min}^{-1}$  for 4-coumaroyl-CoA, with respect to the benzalacetone-forming activity. It is remarkable that the  $K_M$  value remained at a similar level in the point mutant, despite the significant decrease of the  $k_{\text{cat}}$  value. This suggests that the single amino acid replacement mainly affects the catalytic process, rather than the substrate binding to the active-site of the enzyme. It should be noted that when the two mutations, L132T and I214L/L215F, were combined,

the L132T/I214L/L215F triple mutation did not improve the chalcone-forming activity, but instead resulted in a significant loss of activity (Fig. 4).<sup>19</sup>

In addition, the chalcone-forming L132T mutant showed broad substrate specificity.<sup>24</sup> The enzyme also accepted benzoyl-CoA as the starter substrate to produce a trace amount of 2,4,6-trihydroxybenzophenone, after condensations of benzoyl-CoA with three molecules of malonyl-CoA, along with benzoate-primed triketide and tetraketide pyrones as major products, as in the case of the previously reported CHS from *Scutellaria baicalensis*.<sup>24</sup> On the other hand, when phenylacetyl-CoA was used as the starter substrate, the mutant produced only phenylacetate-primed triketide and tetraketide pyrones. In contrast, the wild-type BAS produced only triketide pyrones from benzoyl-CoA and phenylacetyl-CoA starter substrates. These observations suggest that the active-site cavity of the BAS L132T mutant is large enough to accommodate the tetraketide products as in the case of CHS.

Interestingly, the replacement of Leu132 with bulky aromatic residues, Phe, Tyr and Trp, caused a 1.2-fold increase in the benzalacetone-forming activity at pH 8.0, whereas the BNY-forming activity was retained or significantly decreased at pH 6.5 (Fig. 4). These point mutations thus resulted in increased product specificity for the diketide benzalacetone formation, in sharp contrast to the aforementioned large-to-small substitutions. On the other hand, it was quite surprising that the substitution of Leu132 with the small Gly residue did not significantly affect the enzyme activity (Fig. 4). In the crystal structure of the wild-type BAS, Leu132 is located within a loop region. It is tempting to speculate that the Leu to Gly substitution may retain the flexibility of the loop, thereby maintaining a similar active-site structure to that of the wild-type enzyme. In contrast, when Leu132 was substituted with the cyclized and less flexible Pro, the L132P mutant exhibited drastically decreased benzalacetone- and BNY-forming activities (Fig. 4). This result also suggests that the flexibility of the loop structure is important for the enzyme activity.

To further clarify the structure-function relationship, homology models of the L132T and L132W mutants were constructed on the basis of the crystal structure of the wild-type *R. palmatum* BAS (PDB code: 3A5Q),<sup>25</sup> and their active-site architectures were compared with those of the wild-type and the chalcone-producing I214L/L215F double mutant of BAS<sup>7</sup>, and the *Medicago sativa* CHS<sup>8</sup> (Fig. 3). The homology models predicted that the L132T mutant restored the 'coumaroyl binding pocket' in the active-site cavity (Fig. 3d). The total cavity volume of the L132T mutant is estimated to be 400 Å<sup>3</sup>, which is slightly larger than that of the wild-type (350 Å<sup>3</sup>) and almost as large as that of the I214L/L215F mutant (400 Å<sup>3</sup>), but much smaller than that of the *M. sativa* CHS (750 Å<sup>3</sup>). As previously proposed by Noel and Schröder, Thr132 in CHS forms a hydrogen bond with the neighboring Glu192, and is thought to control the folding of the tetraketide intermediate so that the Claisen-type cyclization produces the chalcone scaffold.<sup>10</sup> These observations suggest that the L132T substitution opens a gate to the buried 'coumaroyl-binding pocket', thereby increasing the polyketide chain elongation by up to three condensations with malonyl-CoA, and leading to the formation of chalcone. On the other hand, in the L132W mutant, the replacement of Leu132 with the bulky Trp further blocks the entrance of the pocket. In this case, the total cavity volume is estimated to be 300 Å<sup>3</sup>, which is smaller than that of the wild-type enzyme (350 Å<sup>3</sup>), resulting in the interruption BNY formation, and instead improving the specificity for the benzalacetone-forming activity (Fig. 3e).

In summary, we investigated the functional role of the active-site residue Leu132 of *R. palmatum* BAS, on the basis of the X-ray crystal structures. We found that a single amino acid substitution, L132T, restored the chalcone-forming activity of the enzyme. Homology modeling suggested that this is probably caused by

the restoration of the 'coumaroyl binding pocket' in the active-site cavity. These findings provide further insights into the structural details of the catalytic mechanisms of the type III PKS enzymes.

## Acknowledgments

This work was supported in part by a Grant-in-Aid for Scientific Research from the Ministry of Education, Culture, Sports, Science and Technology, Japan (to I.A. and H.M.), and grants from The Naito Foundation (to I.A.) and Takeda Science Foundation (to H.M.).

## References and notes

- Abe, I.; Morita, H. *Nat. Prod. Rep.* **2010**, *27*, 809.
- Austin, M. B.; Noel, J. P. *Nat. Prod. Rep.* **2003**, *20*, 79.
- Schröder, J. In *Comprehensive Natural Products Chemistry*; Elsevier: Oxford, 1999; Vol. 1. p 749.
- Abe, I.; Takahashi, Y.; Morita, H.; Noguchi, H. *Eur. J. Biochem.* **2001**, *268*, 3354.
- Abe, I.; Sano, Y.; Takahashi, Y.; Noguchi, H. *J. Biol. Chem.* **2003**, *278*, 25218.
- Abe, T.; Morita, H.; Noma, H.; Kohno, T.; Noguchi, H.; Abe, I. *Bioorg. Med. Chem. Lett.* **2007**, *17*, 3161.
- Morita, H.; Shimokawa, Y.; Tanio, M.; Kato, R.; Noguchi, H.; Sugio, S.; Kohno, T.; Abe, I. *Proc. Natl. Acad. Sci. U.S.A.* **2010**, *107*, 669.
- Ferrer, J. L.; Jez, J. M.; Bowman, M. E.; Dixon, R. A.; Noel, J. P. *Nat. Struct. Biol.* **1999**, *6*, 775.
- Jez, J. M.; Austin, M. B.; Ferrer, J.; Bowman, M. E.; Schröder, J.; Noel, J. P. *Chem. Biol.* **2000**, *7*, 919.
- Austin, M. B.; Bowman, M. E.; Ferrer, J. L.; Schröder, J.; Noel, J. P. *Chem. Biol.* **2004**, *11*, 1179.
- Austin, M. B.; Izumikawa, M.; Bowman, M. E.; Udway, D. W.; Ferrer, J. L.; Moore, B. S.; Noel, J. P. *J. Biol. Chem.* **2004**, *279*, 45162.
- Sankaranarayanan, R.; Saxena, P.; Marathe, U. B.; Gokhale, R. S.; Shanmugam, V. M.; Rukmini, R. *Nat. Struct. Mol. Biol.* **2004**, *11*, 894.
- Morita, H.; Kondo, S.; Oguro, S.; Noguchi, H.; Sugio, S.; Abe, I.; Kohno, T. *Chem. Biol.* **2007**, *14*, 359.
- Shomura, Y.; Torayama, I.; Suh, D. Y.; Xiang, T.; Kita, A.; Sankawa, U.; Miki, K. *Proteins* **2005**, *60*, 803.
- Goyal, A.; Saxena, P.; Rahman, A.; Singh, P. K.; Kasbekar, D. P.; Gokhale, R. S.; Sankaranarayanan, R. *J. Struct. Biol.* **2008**, *162*, 411.
- Rubin-Pitel, S. B.; Zhang, H.; Vu, T.; Brunzelle, J. S.; Zhao, H.; Nair, S. K. *Chem. Biol.* **2008**, *15*, 1079.
- Jez, J. M.; Ferrer, J. L.; Bowman, M. E.; Dixon, R. A.; Noel, J. P. *Biochemistry* **2000**, *39*, 890.
- Abe, I.; Watanabe, T.; Morita, H.; Kohno, T.; Noguchi, H. *Org. Lett.* **2006**, *8*, 499.
- Site-directed mutagenesis: The plasmids expressing the BAS mutants (L132G, L132A, L132T, L132S, L132C, L132F, L132Y, L132W, and L132P) were constructed with a QuikChange Site-Directed Mutagenesis Kit (Stratagene), according to the manufacturer's protocol, using the following pairs of primers (mutated codons are underlined): L132G (5'-CTCATCGTGTGTTGCGGAGCGCGGTGAC-3' and 5'-GTCAACGCCGCGTCCGCAACACACGA-3'), L132A (5'-CTCATCGTGTGTTGCGGAGCGCGGTGAC-3' and 5'-CATGTCAACGCCGCGTCCGCAACACACGATGAG-3'), L132T (5'-CTCATCGTGTGTTGCGGAGCGCGGTGAC-3' and 5'-CATGTCAACGCCGCGTCCGCAACACACGATGAG-3'), L132S (5'-CTCATCGTGTGTTGCGGAGCGCGGTGAC-3' and 5'-GTCAACGCCGCGTCCGCAACACACGATGAG-3'), L132C (5'-CTCATCGTGTGTTGCGGAGCGCGGTGAC-3' and 5'-GTCAACGCCGCGTCCGCAACACACGATGAG-3'), L132F (5'-CTCATCGTGTGTTGCGGAGCGCGGTGAC-3' and 5'-GTCAACGCCGCGTCCGCAACACACGATGAG-3'), L132Y (5'-CTCATCGTGTGTTGCGGAGCGCGGTGAC-3' and 5'-GTCAACGCCGCGTCCGCAACACACGATGAG-3'), L132W (5'-CTCATCGTGTGTTGCGGAGCGCGGTGAC-3' and 5'-GTCAACGCCGCGTCCGCAACACACGATGAG-3'), L132P (5'-CTCATCGTGTGTTGCGGAGCGCGGTGAC-3' and 5'-GTCAACGCCGCGTCCGCAACACACGATGAG-3'). The expression plasmid for the L132T/I214L/L215F triple mutant was also constructed in a similar manner.
- Expression and purification: After confirmation of the sequence, the plasmid was transformed into *E. coli* M15. The cells harboring the plasmid were cultured to an A<sub>600</sub> of 0.6 in LB medium containing 100 µg/mL of ampicillin at 37 °C. Subsequently, 1.0 mM isopropylthio-β-D-galactopyranoside was added to induce protein expression, and the cells were further cultured at 23 °C for 16 h. All of the following procedures were performed at 4 °C. The *E. coli* cells were harvested by centrifugation at 5000g, and were resuspended in 50 mM Tris-HCl buffer (pH 8.0), containing 0.2 M NaCl, 5% (v/v) glycerol and 2 mM DTT (buffer A). The cells were disrupted by sonication, and the lysate was centrifuged at 12,000g for 30 min. The supernatant was loaded onto a Glutathione Sepharose 4B affinity column (GE Healthcare) equilibrated with buffer A, and the column was then washed with buffer A. The GST-tag was cleaved on the column by PreScission Protease (GE Healthcare) overnight, and then the recombinant BAS mutant was eluted with buffer A. The resultant BAS protein thus contains three additional residues (Gly-Pro-Gly) at the N-terminal flanking region, derived from the PreScission Protease recognition sequence. The protein concentration was determined by the Bradford method (Protein Assay, Bio-Rad) with bovine serum albumin as the standard.

21. **Enzyme reaction:** The reaction mixture contained 54  $\mu\text{M}$  of 4-coumaroyl-CoA (benzoyl-CoA or phenylacetyl-CoA), 108  $\mu\text{M}$  of malonyl-CoA, and 20  $\mu\text{g}$  of the purified enzyme in a final volume of 500  $\mu\text{L}$  of 100 mM KPB buffer (pH 6.5) or Tris–HCl buffer (pH 8.0), containing 1 mM EDTA. Incubations were performed at 30 °C for 20 min and were stopped by the addition of 50  $\mu\text{L}$  of 20% HCl. The products were then extracted with 3 mL of ethyl acetate. The products were separated by reverse-phase HPLC (JASCO 880) on a TSK-gel ODS-80Ts column (4.6  $\times$  150 mm, TOSOH), at a flow rate of 0.8 mL/min. Gradient elution was performed with  $\text{H}_2\text{O}$  and MeOH, both containing 0.1% TFA: 0–5 min, 30% MeOH; 5–17 min, linear gradient from 30% to 60% MeOH; 17–25 min, 60% MeOH; 25–27 min, linear gradient from 60% to 70% MeOH. Elutions were monitored by a multichannel UV detector (MULTI 340, JASCO) at 280; UV spectra (198–400 nm) were recorded every 0.4 s. Online LC–ESIMS spectra were measured with an Agilent Technologies HPLC 1100 series HPLC coupled to a Bruker Daltonics Esquire4000 ion trap mass spectrometer fitted with an ESI source. HPLC separations were performed under the same conditions as described above. The ESI capillary temperature and the capillary voltage were 320 °C and 4.0 V, respectively. The tube lens offset was set at 20.0 V. All spectra were obtained in the positive mode, over a mass range of  $m/z$  50–500, and at a range of one scan every 0.2 s. The collision gas was helium, and the relative collision energy scale was set at 30.0% (1.5 eV).
22. 4-Coumaroyl-CoA was chemically synthesized as described: Stöckigt, J.; Zenk, M. H. Z. *Naturforsch., C: Biosci.* **1975**, 30, 352 [ $2\text{-}^{14}\text{C}$ ]Malonyl-CoA was purchased from GE Healthcare. Benzoyl-CoA, phenylacetyl-CoA and malonyl-CoA were purchased from Sigma.
23. **Enzyme kinetics:** Steady-state kinetic parameters were determined by using [ $2\text{-}^{14}\text{C}$ ]malonyl-CoA (1.8 mCi/mmol) as the substrate. The experiments were performed in triplicate using four concentrations of 4-coumaroyl-CoA (27.0, 13.5, 6.8, and 3.4  $\mu\text{M}$ ) in the assay mixture, containing 108  $\mu\text{M}$  of malonyl-CoA, 20  $\mu\text{g}$  of purified enzyme, and 1 mM EDTA, in a final volume of 500  $\mu\text{L}$  of 100 mM potassium phosphate buffer, pH6.5. The reactions were incubated at 30 °C for 20 min. The reaction products were extracted and separated by TLC (Merck Art. 1.11798 Silica Gel 60 F254; ethyl acetate/hexane/AcOH = 63:27:5, v/v/v). Radioactivities were quantified by autoradiography using a bioimaging analyzer BAS-2000II (FUJIFILM). Lineweaver–Burk plots of data were employed to derive the apparent  $K_M$  and  $k_{\text{cat}}$  values (average of triplicates), using the EnzFitter software (BIOSOFT).
24. Morita, H.; Takahashi, Y.; Noguchi, H.; Abe, I. *Biochem. Biophys. Res. Commun.* **2000**, 279, 190.
25. **Homology modeling:** The models of the BAS L132T and L132W were generated by the SWISS-MODEL package (<http://expasy.ch/spdbv/>) provided by the Swiss-PDB-Viewer program (Guex, N.; Peitsch, M. C. *Electrophoresis* **1997**, 18, 2714) based on the crystal structure of wild-type BAS (PDB code: 3A5Q). The model quality was assessed using PROCHECK (Liang, J.; Edelsbrunner, H.; Woodward, C. *Protein Sci.* **1998**, 7, 1884). In the Ramachandran plot calculated for the model, most of the amino acid residues were present in the energetically allowed regions with only a few exceptions, primarily Gly residues that can adopt phi/psi angles in all four quadrants. The cavity volume was calculated by the program CASTP (<http://cast.engr.uic.edu/cast/>). All protein structure figures were prepared with PYMOL (DeLano Scientific, <http://www.pymol.org>).